ISSN 1070-3284, Russian Journal of Coordination Chemistry, 2015, Vol. 41, No. 4, pp. 274–284. © Pleiades Publishing, Ltd., 2015.

Synthesis, Crystal Structures, Luminescent Properties, Theoretical Calculation, and DNA Interaction of the Cadmium(II) and Lead(II) Complexes with *o*-Aminobenzoic Acid and 1,10-Phenanthroline[1]

Z. Y. Zhang, C. F. Bi, Y. H. Fan*, X. C. Yan, X. Zhang, P. F. Zhang, and G. M. Huang

Key Laboratory of Marine Chemistry Theory and Technology, Ministry of Education, College of Chemistry and Chemical Engineering, Ocean University of China, Qingdao, Shandong, 266100 P.R. China

**e-mail: fyh1959@163.com; fanyh@ouc.edu.cn*

Received August 27, 2014

Abstract—Two complexes, namely [Cd(Phen)(*o*-AB)$_2$] (**I**) and [Pb(Phen)(*o*-AB)] (**II**) (Phen = 1,10-phenanthroline, *o*-AB = *o*-aminobenzoic acid), have been synthesized and characterized by elemental analysis and X-ray diffraction single-crystal analysis (CIF files CCDC nos. 910307 (**I**), 898292 (**II**)). Complex **I** is six coordinated by two nitrogen and four oxygen atoms from the Phen and *o*-AB to furnish a distorted octahedral geometry. Complex **II** is six coordinated by two nitrogen and four oxygen atoms from the Phen and *o*-AB to furnish an umbrella-like geometry. The complexes exhibit intense fluorescence at room temperature. The interaction between complex **I** and calf thymus DNA was also investigated by UV absorption spectra, fluorescence emission spectra and viscometry. The nature of the binding seems to be mainly an electrostatic interaction between DNA and complex **I**. Theoretical studies of the title complexes were carried out by density functional theory (DFT) B3LYP method.

DOI: 10.1134/S1070328415030094

INTRODUCTION

Heterocyclic compounds are widely distributed in nature and essential to many biochemical processes. These compounds are worth attention for many reasons, chief among them are their biological activities; many drugs are heterocycles [1, 2]. 1,10-Phenanthroline (Phen) and its substituted derivatives, both in the metal-free state and as ligands coordinated to transition metals, disturb the functioning of a wide variety of biological systems [3–5]. When the metal-free *N*,*N*-chelating bases are found to be bioactive, it is usually assumed that the sequestering of trace metals is involved, and that the resulting metal complexes are the actual active species [6–9]. Interests in aminobenzoic acids arise from both their biological importance and their chemical properties. *o*-Aminobenzoic acid, also named anthranilic acid, has been used as a convenient fluorescence probe in internally quenched fluorescent peptides due to its high quantum yield and small size. *o*-Aminobenzoic acid (*o*-AB) is also multifunctional hydrogen-bonding molecules [10–12].

In the viewpoint of constructing functional compounds, the title cadmium(II) and lead(II) complexes were synthesized in anhydrous solvent and their crystal structures were determined. The interaction between complex **I** and calf thymus DNA was also investigated by UV absorption spectra, fluorescence emission spectra and viscometry [13]. Based on crystal data, density functional theory (DFT) studies of the title complexes were performed using the Gaussian 03 program suite. The natural atomic charges distribution, molecular total energy and frontier molecular orbital energies of the complexes were discussed [14].

EXPERIMENTAL

Materials and physical measurement. Calf thymus DNA (CT-DNA) were obtained from Sigma-Aldrich Co. (USA). The other reagents used in this work were of analytical grade. The experiments involving interaction of the complexes with CT-DNA were carried out in Milli-Q water buffer containing 5 mM Tris and 50 mM NaCl, and adjusted to pH 7.2 with hydrochloric acid. A solution of CT-DNA gave a ratio of UV absorbance at 260 and 280 nm of about 1.8–1.9, indicating that the CT-DNA was sufficiently free of protein [15]. The CT-DNA concentration per nucleotide was determined spectrophotometrically by employing an extinction coefficient of 6600 L mol^{-1} cm^{-1} at 260 nm [16].

Elemental analyses were carried out with a model 2400 PerkinElmer analyzer. The fluorescence spectra were recorded on an F-4500 fluorimeter. The X-ray diffraction data were collected on a Bruker Smart CCD X-ray single-crystal diffractometer. Viscosity

[1] The article is published in the original.

measurements were conducted using an Ubbelodhe viscometer. Optimizations of geometrical structures and Natural Bond Orbital (NBO) analyses of the title complexes were carried out by DFT B3LYP method. The 6–31 + G* basis set was used for C, N and O atoms, while the effective core potential (ECP) and valence double-ζ LANL2DZ basis set was used for Pb and Cd atom [17, 18]. Atom coordinates used in the calculations were from crystallographic data, and a molecule in the unit cells was selected as the initial model. All calculations were conducted on a Pentium IV computer using Gaussian 03 program [19].

Synthesis of complexes. *o*-AB (2.0 mmol) was dissolved in 50 mL of anhydrous methanol. $M(OAc)_2 \cdot nH_2O$ (M = Cd(II) and Pb(II)) (1.0 mmol) dissolved in 30 mL of anhydrous methanol was added dropwise to the above *o*-AB solution and stirred for 4 h at 55°C. Then Phen (1.0 mmol) dissolved in 10 mL of anhydrous methanol was added dropwise to the above solution and stirred for 4 h at 55°C cooled and filtered. The filtrate was left for slow evaporation at room temperature. The wine prismatic crystals were formed 20 days later.

For $C_{26}H_{20}N_4O_4Cd$ (**I**)

anal. calcd., %:	C, 55.28;	H, 3.56;	N, 9.92.
Found, %:	C, 55.35;	H, 3.68;	N, 9.83.

For $C_{26}H_{20}N_4O_4Pb$ (**II**)

anal. calcd., %:	C, 47.34;	H, 3.06;	N, 8.49.
Found, %:	C, 47.30;	H, 3.12;	N, 8.50.

X-ray structure determination. All data were collected on a Bruker Smart CCD X-raysingle-crystal diffractometer at 298(2) K with a graphite-monochromated MoK_α radiation (λ = 0.71073 Å) by using an ω–2θ scan mode. The structure was solved by direct methods using SHELXS-97 [20]. The non-hydrogen atoms were defined with Fourier synthesis method. Positional and thermal parameters were refined by fullmatrix least-squares method to convergence. A summary of the key crystallographic information is given in Table 1. Selected bond lengths and bond angles of complexes **I** and **II** are listed in Table 2. Hydrogen bond geometry of the complexes is listed in Table 3. Crystal structure of the title complexes are depicted in Fig. 1. Packing diagrams of the title complexes are depicted in Fig. 2.

Supplementary material has been deposited with the Cambridge Crystallographic Data Centre (nos. 910307 (**I**), 898292 (**II**); deposit@ccdc.cam.ac.uk or http://www.ccdc.cam.ac.uk).

Fluorescence properties. The fluorescence spectra of the complexes and the ligands were carried out in methanol solution. For complex **I**, the sample was excited at 319 nm. The scanner speed was 240 nm min^{-1} and the slit width was 2.5 nm. For complex **II**, the sample was excited at 314 nm. The scanner speed was 240 nm min^{-1} and the slit width was 2.5 nm.

DNA-binding studies were carried out by ultraviolet (a) and fluorescence (b) spectra and viscosity measurements (c). **a**. Complex **I** was dissolved in a mixture of DMSO and Tris–HCl buffer. Absorption titration experiments were carried out by gradually increasing the DNA concentration and maintaining the complexes concentration at 5.75×10^{-7} M. Absorbances were recorded after each successive addition of DNA solution and equilibration.

b. For complex **I**, spectral measurements was carried out by successive additions of DNA ($0.0–3.78 \times 10^{-5}$ mol/L) to the complex **I** (1.51×10^{-5} mol/L) in Tris–HCl buffer. The sample was excited at 319 nm. The scanner speed was 240 nm min^{-1} and the slit width was 2.5 nm.

c. Viscosity measurements were conducted using an Ubbelodhe viscometer, which was immersed in a thermostated water bath maintained to 298 (±0.1) K. Titrations were performed for the complex which can be introduced into a DNA solution in the viscometer. Data were presented as $(\eta/\eta_0)^{1/3}$ versus the ratio of the concentration of the complex and DNA, where η is the viscosity of DNA in the presence of the complex and η_0 is the viscosity of DNA alone.

RESULTS AND DISCUSSION

As shown in Fig. 1a, in complex **I**, Cd(II) atom is located in a very distorted octahedral coordination with six bonds to two N atoms from one Phen and four carboxylate O atoms from two *o*-AB ligands. There are two four-membered chelate rings (Cd(1)–O(1)–C(1)–O(2), Cd(1)–O(3)–C(8)–O(4)) and one five-membered chelate ring (Cd(1)–N(3)–C(19)–C(20)–N(4)). As shown in Fig. 1b, in complex **II**, Pb(II) atom is located in a very distorted octahedral coordination with six bonds to two N atoms from one Phen and four carboxylate O atoms from two *o*-AB ligands. There are two four-membered chelate rings (Pb(1)–O(1)–C(1)–O(2), Pb(1)–O(3)–C(8)–O(4)) and one five-membered chelate ring (Pb(1)–N(3)–C(19)–C(20)–N(4)). But the geometry of complex **II** is different from the complex **I**, which forms an umbrella-like geometry in which Pb(1)–O(1) bond serves as the umbrella handle.

As shown in Fig. 2a and Table 3, complex **I** forms two intermolecular hydrogen bonds N(1)–H(1*A*)···O(1) and N(2)–H(2*B*)···O(3) between the exocyclic amine group and the oxygen atom of the carboxyl group. The molecules are linked into extended chains parallel to the *y* axis and the *z* axis through the involving intermolecular N–H···O hydrogen bonds. A three-dimensional network is assembled through van der Waals' forces and intermolecular π–π interactions [21, 22].

As shown in Fig. 2b and Table 3, complex **II** forms two intermolecular hydrogen bonds N(1)–H(1*B*)···O(2) and N(2)–H(2*B*)···O(3) between the exocyclic amine

Table 1. Crystallographic data and structure refinement for complexes **I** and **II**

Parameter	Value	
	I	**II**
Fw	564.86	659.65
Crystal system	Monoclinic	Triclinic
Space group	$P2_1/c$	$P\bar{1}$
a, Å	7.6462(6)	7.8127(6)
b, Å	17.1758(17)	12.9880(11)
c, Å	17.7436(18)	13.4150(12)
α, deg	90	63.4960(10)
β, deg	100.1000(10)	84.243(2)
γ, deg	90	77.5180(10)
Volume, Å^3	2294.1(4)	1189.37(17)
Z	4	2
ρ_{calcd}, g/cm^3	1.635	1.842
μ, mm^{-1}	0.994	7.133
F(000)	1136	636
Crystal size, mm	0.43 × 0.40 × 0.21	0.40 × 0.35 × 0.18
θ Range for data collection, deg	2.62–25.02	2.67–25.01
Limiting indices	$-9 \le h \le 8$,	$-7 \le h \le 9$,
	$-17 \le k \le 20$,	$-14 \le k \le 15$,
	$-18 \le l \le 21$	$-12 \le l \le 15$
Reflections collected/unique (R_{int})	11313/4037 (0.0375)	5941/4125 (0.0308)
Completeness to θ = 25.01, %	99.6	98.2
Max and min transmission	0.8185 and 0.6746	0.3600 and 0.1626
Refined parameters	316	317
Goodness of fit on F^2	1.035	1.073
Final *R* indices ($I > 2\sigma(I)$)	$R_1 = 0.0360$, $wR_2 = 0.0851$	$R_1 = 0.0388$, $wR_2 = 0.0987$
R indices (all data)	$R_1 = 0.0520$, $wR_2 = 0.0944$	$R_1 = 0.0437$, $wR_2 = 0.1016$
Largest diff. peak and hole, *e* Å^{-3}	0.659 and −0.425	2.613 and −3.083

Table 2. Selected bond lengths (Å) and angles of the complexes **I** and **II** obtained from experiment and calculations

I			**II**		
Bond	*d*, Å		Bond	*d*, Å	
	Exp.	Calcd.		Exp.	Calcd.
Cd(1)–O(3)	2.390(3)	2.34749	Pb(1)–O(3)	2.494(5)	2.42703
Cd(1)–O(1)	2.438(3)	2.34731	Pb(1)–O(1)	2.347(4)	2.24129
Cd(1)–N(4)	2.335(3)	2.45699	Pb(1)–N(4)	2.632(6)	2.89141
Cd(1)–N(3)	2.318(3)	2.45707	Pb(1)–N(3)	2.591(6)	2.76720
Cd(1)–O(2)	2.246(3)	2.30410	Pb(1)–O(2)	2.600(5)	2.58426
Cd(1)–O(4)	2.251(3)	2.30378	Pb(1)–O(4)	2.699(6)	2.43615
N(1)–C(3)	1.327(7)	1.38149	N(1)–C(3)	1.371(9)	1.38044
N(2)–C(10)	1.363(5)	1.38149	N(2)–C(10)	1.363(10)	1.38440
N(3)–C(15)	1.330(5)	1.32766	N(3)–C(15)	1.322(10)	1.32852
N(3)–C(19)	1.362(5)	1.35519	N(3)–C(19)	1.376(10)	1.35787
N(4)–C(24)	1.320(5)	1.32766	N(4)–C(24)	1.302(11)	1.32651
N(4)–C(20)	1.357(4)	1.35517	N(4)–C(20)	1.369(10)	1.35437
O(1)–C(1)	1.253(5)	1.28648	O(1)–C(1)	1.293(8)	1.28941
O(2)–C(1)	1.254(4)	1.27396	O(2)–C(1)	1.254(8)	1.27149
O(3)–C(8)	1.250(5)	1.28646	O(3)–C(8)	1.266(9)	1.29057
O(4)–C(8)	1.266(4)	1.27400	O(4)–C(8)	1.264(8)	1.26937
C(1)–C(2)	1.489(5)	1.48915	C(1)–C(2)	1.481(10)	1.48430
C(8)–C(9)	1.480(5)	1.48915	C(8)–C(9)	1.498(10)	1.48878
Angle	Exp.	Calcd.	Angle	Exp.	Calcd.
O(3)Cd(1)O(1)	100.26(11)	123.36058	O(3)Pb(1)O(1)	81.55(18)	82.36694
O(3)Cd(1)N(4)	99.31(11)	86.62506	O(3)Pb(1)N(4)	139.70(19)	131.10566
O(1)Cd(1)N(4)	148.37(11)	147.67536	O(1)Pb(1)N(4)	81.61(19)	75.82066
O(3)Cd(1)N(3)	153.74(10)	147.63932	O(3)Pb(1)N(3)	77.45(18)	76.63667
O(1)Cd(1)N(3)	98.94(10)	86.62591	O(1)Pb(1)N(3)	80.11(17)	85.23672
N(4)Cd(1)N(3)	72.26(11)	68.12393	N(4)Pb(1)N(3)	63.7(2)	58.57932
O(3)Cd(1)O(2)	92.45(10)	109.56513	O(3)Pb(1)O(2)	117.95(16)	127.05507
O(1)Cd(1)O(2)	55.20(10)	56.94478	O(1)Pb(1)O(2)	52.59(14)	54.05367
N(4)Cd(1)O(2)	99.44(10)	104.69721	N(4)Pb(1)O(2)	78.17(18)	74.89720
N(3)Cd(1)O(2)	113.26(10)	96.63468	N(3)Pb(1)O(2)	123.04(17)	124.83402
O(3)Cd(1)O(4)	55.82(9)	56.84317	O(3)Pb(1)O(4)	50.07(15)	54.10703
O(1)Cd(1)O(4)	105.79(10)	109.60128	O(1)Pb(1)O(4)	79.22(18)	86.32714
N(4)Cd(1)O(4)	105.74(11)	96.51089	N(4)Pb(1)O(4)	156.27(19)	159.50556
N(3)Cd(1)O(4)	101.61(10)	104.58388	N(3)Pb(1)O(4)	125.62(18)	130.70270

Table 3. Geometric parameters of hydrogen bonds of complexes **I** and **II***

D–H···A	Distance, Å			Angle D–H···A, deg
	D–H	H···A	D···A	
I				
N(1)–H(1*A*)···O(1)	0.86	2.08	2.719 (6)	131.0
N(2)–H(2*A*)···O(1)^{iv}	0.86	2.36	3.189 (4)	163.0
N(2)–H(2*B*)···O(3)	0.86	2.04	2.678 (4)	131.0
C(7)–H(7)···O(2)	0.93	2.41	2.730 (6)	100.0
C(13)–H(13)···O(3)^{i}	0.93	2.56	3.434 (5)	156.0
C(14)–H(14)···O(2)^{i}	0.93	2.52	3.279 (5)	139.0
C(14)–H(14)···O(4)	0.93	2.45	2.774 (5)	100.0
C(25)–H(25)···O(2)^{iii}	0.93	2.56	3.189 (5)	126.0
C(25)–H(25)···O(4)^{iii}	0.93	2.57	3.318 (6)	138.0
II				
N(1)–H(1*A*)···O(4)^{ii}	0.86	2.24	3.056 (9)	158.0
N(1)–H(1*B*)···O(2)	0.86	2.07	2.699 (9)	130.0
N(2)–H(2*A*)···O(1)^{ii}	0.86	2..22	3.015 (9)	154.0
N(2)–H(2*B*)···O(3)	0.86	2.08	2.701 (9)	129.0
C(4)–H(4)···O(4)^{ii}	0.93	2.57	3.354 (12)	142.0
C(6)–H(6)···O(2)^{i}	0.93	2.49	3.409 (11)	172.0
C(7)–H(7)···O(1)	0.93	2.46	2.790 (10)	101.0
C(14)–H(14)···O(4)	0.93	2.49	2.808(10)	100.0
C(15)–H(15)···O(3)	0.93	2.35	3.038 (10)	131.0
C(26)–H(26)···N(1)^{ii}	0.93	2.60	3.489(13)	160.0

Symmetry codes: ^{i} x, y, z; ^{ii} $-x, y + 1/2, -z + 1/2$; ^{iii} $-x, -y, -z$; ^{iv} $x, -y - 1/2, z - 1/2$ (for **I**); ^{i} x, y, z; ^{ii} $-x, -y, -z$ (for **II**).

group and the oxygen atom of the carboxyl group. The molecules are linked into extended chains parallel to the *z* axis through the involving intermolecular N–H···O and C–H···O hydrogen bonds. Adjacent chains are linked into a two-dimensional layer structure through the involving intermolecular N–H···O hydrogen bonds. A three-dimensional network is assembled through short contact between different layers.

The fluorescence spectra of the complexes in methanol solution are shown in Fig. 3. The fluorescence spectra for the complex **I**, *o*-AB ligand and Phen were measured upon the excitation at 319 nm. The intense fluorescence peaks of complex appear at near 393 nm and may be attributed to *o*-AB. The fluorescence spectra for complex **II**, *o*-AB ligand and Phen were measured upon excitation at 314 nm. The intense fluorescence peaks of complex appear at near 395 nm and may be attributed to *o*-AB. The fluorescence intensity of the complexes is highly increased as compared with free Phen [23]. But it is decreased as compared with free *o*-AB.

As shown in Fig. 3, the luminescence of complexes arises from an intra-ligand charge transfer (ILCT) [24, 25]. And the complexes exhibit blue emission. This can be modified by different local ligand environments. The fluorescence intensity of the complexes is it is decreased as compared with free *o*-AB. The reason is that the conjugate intensity of *o*-AB ligand is weaker than free *o*-AB [26, 27].

In the following functional study of the complexes, however, the spectroscopic properties may be available as a suitable indicator reflecting the interaction with biological or chemical substances such as proteins, nucleic acids or other ligands in solution.

Comparison of bond lengths and angles of complexes **I** and **II** obtained from experiment and calculation is made in Table 2. The results indicate that some bond lengths and bond angles obtained from the calculations are agree with those gained from the determination. As shown in Table 2, the corresponding calculated bond lengths of the three ligands in complexes are nearly equal, although limited by the accuracy of the method, their experimental values are not equal.

The energies and components of molecular orbital are important characteristics in theoretical studies, which can predict the chemical properties [28–30]. Some frontier molecular orbital energies and components of complexes are given in Table 4. View of the frontier molecular orbital of complexes is shown in Fig. 4. For the complex **I**, the total energy is –1570.996 a.u. The energies of HOMO, HOMO-1 and HOMO-2 orbital are –0.196, –0.199 and –0.242 a.u., respectively. The energies of LUMO, LUMO+1 and LUMO+2 orbital are –0.096, –0.092 and –0.050 a.u., respectively. The energy gap between HOMO and LUMO orbital is 0.100 a.u. The dipole moment is 8.4636 D. The energies of the molecular, HOMO, LUMO and their neighboring orbital are all

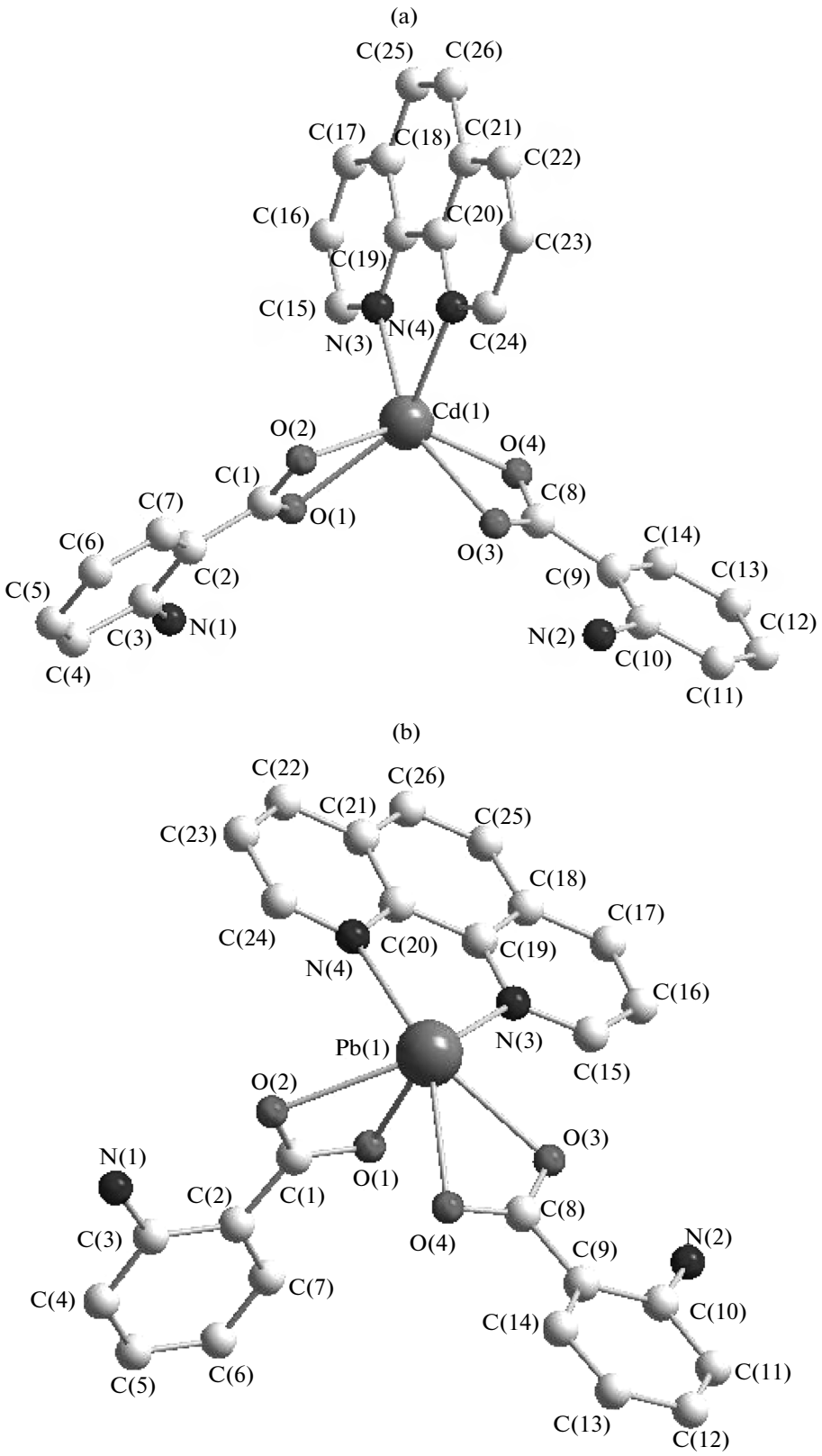

Fig. 1. The structures of complexes **I** (a) and **II** (b).

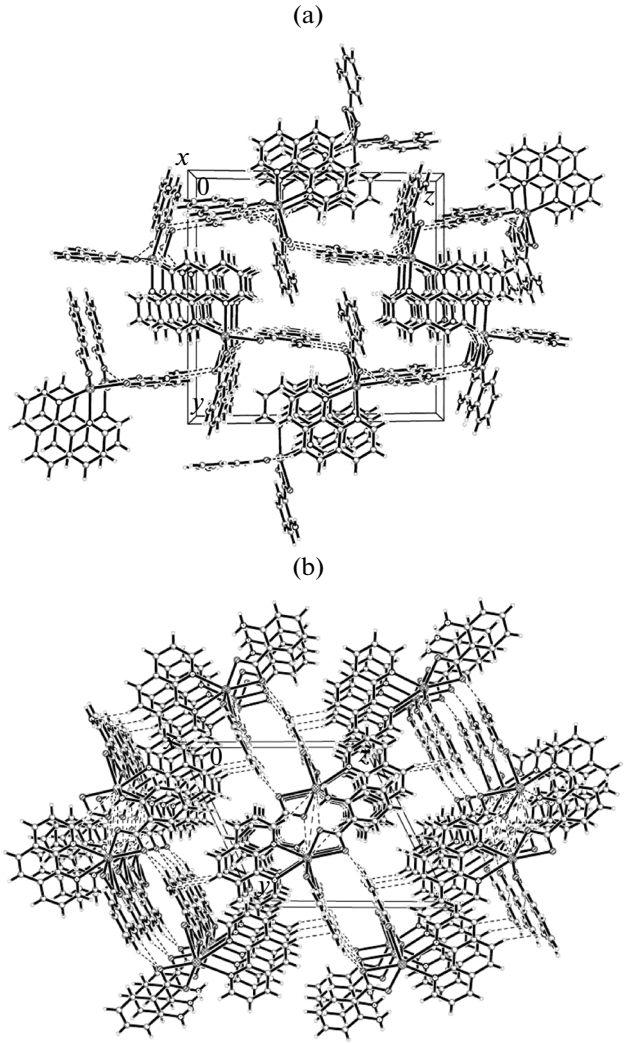

Fig. 2. Packing diagram of the unit cell of complex **I** (a) and **II** (b) viewed along *x* axis. Hydrogen bonds are shown as dashed lines.

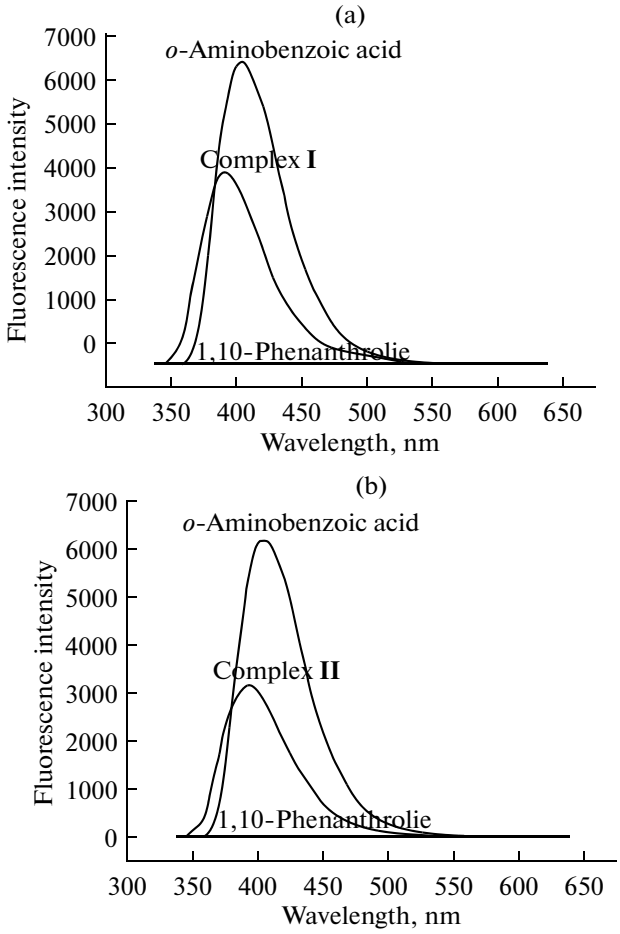

Fig. 3. Fluorescence spectra of complexes **I** (a), **II** (b), free Phen and free *o*-AB in the methanol solution. The concentration of each ligand and complex is 8.0×10^{-5} mol/L. The excitation wavelength of complexes: 319 (**I**), 314 nm (**II**).

negative, indicating that the complex is stable. For the complex **II**, the total energy is −1526.405 a.u. The energies of HOMO, HOMO-1 and HOMO-2 orbital are −0.197, −0.200 and −0.235 a.u., respectively. The energies of LUMO, LUMO+1 and LUMO+2 orbital are −0.086, −0.083 and −0.041 a.u., respectively. The energy gap between HOMO and LUMO orbital is 0.111 a.u. The dipole moment is 8.7253 D. The energies of the molecular, HOMO, LUMO and their neighboring orbital are all negative, indicating that the complex is stable [31–33].

Geometrical structure of the complex is related to the distribution of natural atomic charge. Table 5 indicates part natural atomic charges of the complexes. Natural atomic charge data show that all O and N atoms carry negative charges, the C atoms linking with O and N atoms carry positive charges, and the C atoms linking with H atoms carry negative charges. These negative charged O and N atoms are easy to coordinate with the positive charged metal ion. For complex **I**, the charge of Cd(II) decreases from +2 to +1.487, which indicates that part of the electrons have transferred from N and O atoms to Cd^{2+} ion and the stable Cd(II) complex was formed. For complex **II**, the charge of Pb(II) decreases from +2 to +1.481, which indicates that part of the electrons have transferred from N and O atoms to Pb^{2+} ion and the stable Pb(II) complex was formed.

Electronic absorption spectra are employed to study the binding of complex **I** with CT-DNA. The ultraviolet spectral of the complex with CT-DNA are shown in Fig. 5. In the UV region, the absorption bands at 207 nm for complex **I** can be attributed to π–π* transition of the coordinated ligands. Addition of increasing amounts of CT-DNA results in hyperchromism and slight blue shift of the absorption bands. An electrostatic interaction between CT-DNA and complex **I** can be predicted based on the hyper-

Table 4. Some frontier molecular orbital energies (a.u.) and components (%) of complexes **I** and **II**

Atom	I				Atom	II			
	HOMO-1	HOMO	LUMO	LUMO+1		HOMO-1	HOMO	LUMO	LUMO+1
	energy, a.u.					energy, a.u.			
	−0.196	−0.199	−0.096	−0.092		−0.200	−0.197	−0.186	−0.083
	component, %					component, %			
Cd(1)	0.11	0.33	0.54	0.34	Pb(1)	0.02	0.05	0.07	0.04
N(1)	0.02	20.32	0.00	0.03	N(1)	12.09	0.00	0.03	0.09
N(2)	14.99	0.02	0.00	0.08	N(2)	0.02	5.38	0.01	0.00
N(3)	0.01	0.05	1.66	0.65	N(3)	0.01	0.03	1.36	0.16
N(4)	0.04	0.01	1.20	1.44	N(4)	0.18	0.14	1.05	1.14
O(1)	0.01	0.52	0.05	0.02	O(1)	0.65	0.02	0.25	0.01
O(2)	0.01	1.09	0.02	0.01	O(2)	0.36	0.01	0.02	0.01
O(3)	0.29	0.02	0.06	0.00	O(3)	0.01	0.12	0.06	0.01
O(4)	0.65	0.01	0.03	0.01	O(4)	0.04	0.38	0.02	0.00
C(1)	1.12	4.84	5.96	0.82	C(1)	3.43	7.54	2.53	0.69
C(2)	0.98	12.15	3.32	7.01	C(2)	8.68	5.79	1.72	13.75
C(3)	1.03	8.20	20.39	10.51	C(3)	4.22	1.34	10.00	8.01
C(4)	0.32	7.96	10.64	0.47	C(4)	4.01	0.79	12.54	5.20
C(5)	0.10	0.78	3.63	0.87	C(5)	1.03	0.14	0.32	0.67
C(6)	0.15	10.50	4.24	2.72	C(6)	6.90	0.45	0.82	0.57
C(7)	0.32	1.95	2.16	1.48	C(7)	2.18	1.34	1.48	1.60
C(8)	9.37	1.07	1.25	0.55	C(8)	0.01	6.08	0.43	0.65
C(9)	12.59	1.27	0.74	12.17	C(9)	0.87	15.43	1.37	4.83
C(10)	16.99	0.95	15.59	9.82	C(10)	1.21	10.06	4.74	2.43
C(11)	6.62	1.67	10.38	3.90	C(11)	0.94	6.87	7.59	4.22
C(12)	1.08	0.09	1.93	0.73	C(12)	0.44	0.89	0.52	0.18
C(13)	8.31	0.23	1.25	0.91	C(13)	3.23	4.15	0.29	2.19
C(14)	3.04	0.86	0.33	3.85	C(14)	2.92	15.67	2.32	12.76
C(15)	0.66	4.62	0.28	2.91	C(15)	0.45	2.11	0.91	4.90
C(16)	1.88	4.80	1.45	0.04	C(16)	2.03	0.01	5.63	5.16
C(17)	0.92	2.32	3.24	2.45	C(17)	8.49	1.33	6.75	6.69
C(18)	2.55	2.72	0.93	3.75	C(18)	3.08	2.79	0.80	2.63
C(19)	4.33	2.44	1.52	5.04	C(19)	8.75	5.26	3.21	3.22
C(20)	4.20	4.59	2.65	5.54	C(20)	6.90	1.42	5.50	3.20
C(21)	2.03	0.52	0.72	2.81	C(21)	8.97	1.55	7.53	0.59
C(22)	0.42	0.17	1.47	4.82	C(22)	1.13	0.81	15.66	6.24
C(23)	0.21	0.13	1.38	2.01	C(23)	0.09	0.25	1.67	3.05
C(24)	0.40	0.11	0.10	3.89	C(24)	0.04	0.00	0.67	2.32
C(25)	1.73	1.28	0.23	2.93	C(25)	5.49	1.59	1.37	1.12
C(26)	2.52	1.40	0.67	5.40	C(26)	1.09	0.18	0.75	1.65

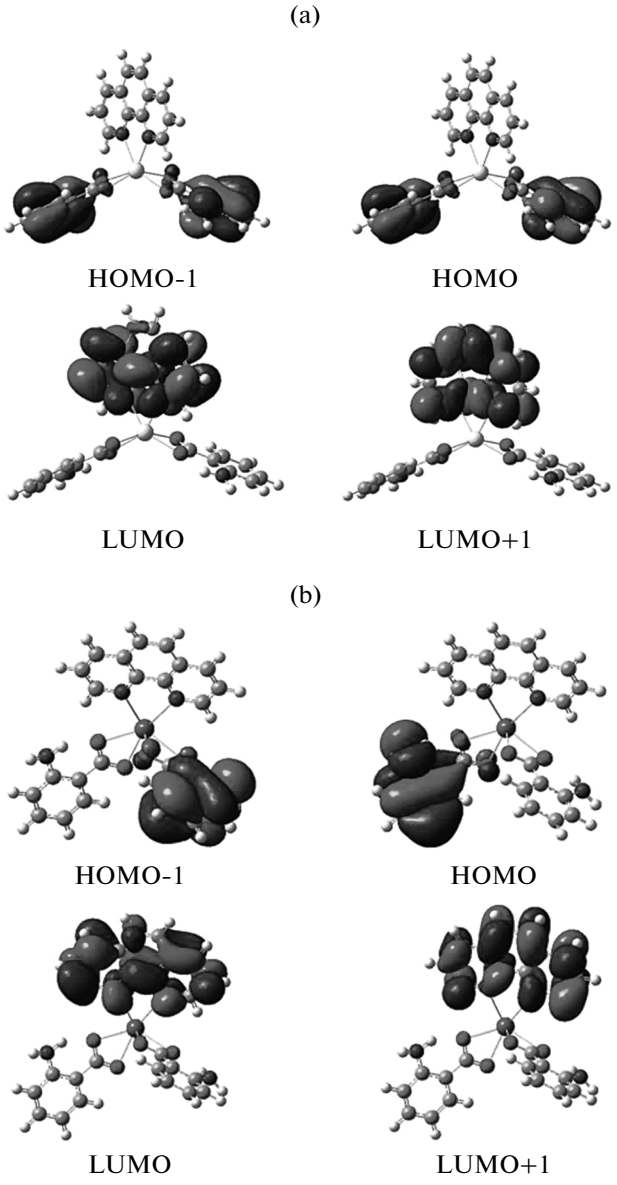

Fig. 4. View of the frontier molecular orbital of complexes **I** (a) and **II** (b).

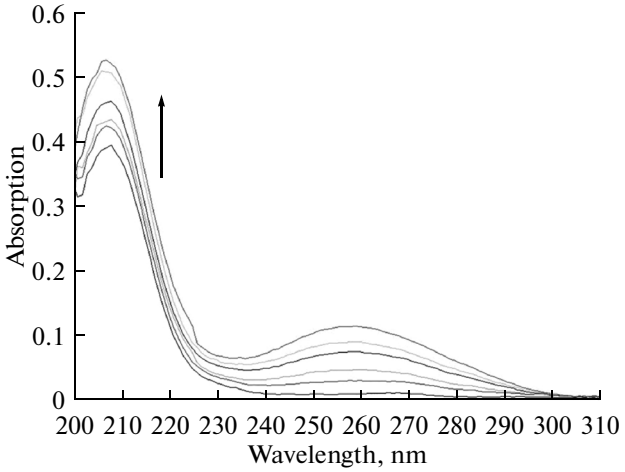

Fig. 5. Absorption spectra of complex **I** in the absence and presence of increasing amounts of DNA. $c_{compl} = 5.75 \times 10^{-7}$ mol/L, $c_{DNA} = 0–1.43 \times 10^{-5}$ mol/L. Arrow shows the absorbance change upon increasing DNA concentration.

chromism exhibited and shift in absorbance. Since each complex has one Phen and two benzene rings, located at different planes, the cadmium complex is non-planar and classical intercalation is precluded [34]. As the DNA double helix possesses many hydrogen bonding sites which are accessible both in the minor and major grooves, it is likely that N–H in benzene ring of the complex forms hydrogen bonds with N of adenine or O of thymine in the DNA [35]. Because, so many Phen and *o*-AB exist in the cadmium complex, it could form hydrogen bonds between aromatic rings of the complex and DNA, contributing to the hyperchromism observed in absorption spectra [36, 37].

Fluorescence spectra are employed to study the binding of complex **I** with CT-DNA. The addition of increasing amounts of CT-DNA results in fluorescence quenching, because there is an electrostatic interaction between the phosphate group of DNA and the complex. The activity and the absorption intensity of the complex decrease due to the large amount of DNA molecule. Thus, the corresponding fluorescence intensity decreases. If it has a classical intercalation between CT-DNA and complex **I**, the complex will be inserted into the base pairs of DNA. The Luminescent groups of complex get into the hydrophobic environment which will make the fluorescence enhancement. So the classical intercalation is precluded.

Viscosity, sensitive to volume increases, is regarded as one of the least ambiguous and most critical tests of binding interactions with DNA in solution in the absence of crystallographic structural data [38]. To further confirm the interaction mode between and complex **I** and DNA, a viscosity study was carried out. Classical intercalation is known to cause a significant increase in the viscosity of a DNA solution, as base pairs are separated to accommodate the binding ligand. In contrast, a partial intercalation mode could bend (or kink) the DNA helix, resulting in decrease of the effective length and viscosity. Other binding causes no obvious increase of DNA viscosity [15, 39].

The specific viscosity of DNA can be considered to remain invariable with increased concentration of **I**, which supports the studies suggesting that the complexes interact with DNA *via* electrostatic interaction mode.

ACKNOWLEDGMENTS

This research was supported by the National Natural Science Foundation of China (grants nos. 21371161 and 21071134), the Specialized Research Fund for the Doctoral Program of Higher Education of China (grant

Table 5. Part natural atomic charges of complexes **I** and **II**

I		II	
Atom	Nature charge	Atom	Nature charge
Cd(1)	1.487	Pb(1)	1.481
N(1)	−0.851	N(1)	−0.849
N(2)	−0.851	N(2)	−0.851
N(3)	−0.511	N(3)	−0.484
N(4)	−0.511	N(4)	−0.486
O(1)	−0.816	O(1)	−0.812
O(2)	−0.751	O(2)	−0.751
O(3)	−0.816	O(3)	−0.833
O(4)	−0.751	O(4)	−0.772
C(1)	0.777	C(1)	0.792
C(2)	−0.217	C(2)	−0.221
C(3)	0.207	C(3)	−0.218
C(4)	−0.294	C(4)	−0.293
C(5)	−0.206	C(5)	−0.203
C(6)	−0.295	C(6)	−0.294
C(7)	−0.173	C(7)	−0.170
C(8)	0.777	C(8)	−0.806
C(9)	−0.217	C(9)	−0.218
C(10)	0.207	C(10)	−0.207
C(11)	−0.294	C(11)	−0.292
C(12)	−0.206	C(12)	−0.205
C(13)	−0.295	C(13)	−0.292
C(14)	−0.173	C(14)	−0.169
C(15)	0.069	C(15)	−0.056
C(16)	−0.273	C(16)	−0.271
C(17)	0.150	C(17)	−0.165
C(18)	−0.112	C(18)	−0.092
C(19)	0.192	C(19)	0.193
C(20)	0.192	C(20)	0.186
C(21)	−0.092	C(21)	−0.096
C(22)	−0.148	C(22)	−0.168
C(23)	−0.270	C(23)	−0.283
C(24)	0.069	C(24)	0.099
C(25)	−0.134	C(25)	−0.209
C(26)	−0.228	C(26)	−0.190

no. 20120132110015), the Natural Science Foundation of Shandong Province (grant no. ZR2012BQ026).

REFERENCES

1. Zhang, L.L., Wang, L.D., Zhan, S.H., et al., *Struct. Chem.*, 2014, vol. 25, p. 103.
2. Zhang, N., Fan, Y.H., Zhang, Z., et al., *Inorg. Chem. Commun.*, 2012, vol. 22, p. 68.
3. Bian, L., Li, L.Z., Zhang, Q.F., et al., *Transition Met. Chem.*, 2012, vol. 37, p. 783.
4. Haribabu, P., Patil, Y.P., Reddy, K.H., and Nethaji, M., *Transition Met. Chem.*, 2011, vol. 36, p. 867.
5. Geraghty, M., McCann, M., Devereux, M., et al., *Met.-Based Drugs*, 1999, vol. 6, p. 41.
6. Dolan, N., McGinley, J., Stephens, J.C., et al., *Inorg. Chim. Acta*, 2014, vol. 409, p. 276.
7. Zhang, Z.Y., Bi, C.F., Fan, Y.H., Zhang, X., Zhang, N., Yan, X.C., Zuo, J., *Bull. Korean Chem. Soc.*, 2014, vol. 35, p. 1697.
8. Sallam, A.A., Ramasahayam, S., Meyer, S.A., and El-Sayed, K.A., *Bioorg. Med. Chem.*, 2010, vol. 18, p.7446.
9. Zhang, F., Zhang, Q.Q., Wang, W.G., and Wang, X.L., *J. Photochem. Photobiol.*, A, 2006, vol. 184, p. 241.
10. He, Y.G., Wu, C.Y., and Kong, W., *J. Phys. Chem.*, 2005, vol. 109, p. 2809.
11. Mohamed, G.G., Omar, M.M., and Hindy, A.M.M., *Spectrochim. Acta, A*, 2005, vol. 62, p.1140.
12. Zhuang, R.R., Jian, F.F., and Wang, K.F., *J. Mol. Struct.*, 2009, vol. 938, p. 254.
13. Darabi, F., Hadadzadeh, H., Ebrahimi, M., et al., *Inorg. Chim. Acta*, 2014, vol. 409, p. 379.
14. Machura, B., Świtlicka, A., Palion, J., and Kruszynski, R., *Struct. Chem.*, 2013, vol. 24, p. 89.
15. Satyanarayana, S., Dabrowiak, J.C., and Chaires, J.B., *Biochemistry*, 1993, vol. 32, p. 2573.
16. Zhang, N., Fan, Y.H., Bi, C.F., et al., *Transition Met. Chem.*, 2013, vol. 38, p. 463.
17. Hariharan, P.C. and Pople, J.A., *Chem. Phys. Lett.*, 1972, vol. 16, p. 217.
18. Kaya, Y. and Yilmaz, V.T., *Struct. Chem.*, 2014, vol. 25, p. 231.
19. Frisch, K.D., Trucks, G.W., Schlegel, H.B., et al., Gaussian03, Revision A. 6, Pittsburgh (PA, USA): Gaussian, Inc., 2003.
20. Sheldrick, G.M., *SHELXTL-97, Program for Crystal Structure Refinement*, Göttingen (Germany): Univ. of Göttingen, 1997.
21. Pschirer, N.G., Ciurtin, D.M., and Smith, M.D., *Angew. Chem.*, 2002, vol. 114, p. 603.
22. Hoog de, P., Gamez, P., Mutikainen, I., et al., *Angew. Chem.*, 2004, vol. 116, p. 5939.
23. Wang, Y. and Okabe, N., *Chem Pharm Bull.*, 2005, vol. 53, p. 645.
24. Zhao, N., Wu, Y.H., Wen, H.M., et al., *Organometallics*, 2009, vol. 28, p. 5603.
25. Fan, R.Q., Zhang, Y.J., Yin, Y.B., et al., *Synth. Met.*, 2009, vol. 159, p. 1106.

26. Leslie, W., Poole, R.A., Murray, P.R., et al., *Polyhedron*, 2004, vol. 23, p. 2769.
27. Jin, J., Wang, X.Y., Li, Y.Y., et al., *Struct. Chem*., 2012, vol. 23, p. 1523.
28. Fleming J., Frontier Orbitals and Organic Chemical Reactions, London: Wiley, 1976.
29. Vijaya Chamundeeswari, S.P., James Jebaseelan Samuel, E., and Sundaraganesan, N., *Spectrochim. Acta, A,* 2014, vol. 118, p. 1.
30. Mansour, A.M., *Inorg. Chim. Acta*, 2013, vol. 408, p. 186.
31. Xia, S.W., Xu, X., Sun, Y.L., et al., *Chin. J. Struct. Chem*., 2006, vol. 25, p. 197.
32. Zhu, Y.Y., Zhao, H.G., Liu, C.M., et al., *Struct. Chem*., 2014, vol. 25, p. 699.
33. Wang, A.D., Bi, C.F., Fan, Y.H., et al., *Russ. J. Coord. Chem*., 2008, vol. 34, p. 475.
34. Carter, M.T., Rodriguez, M., and Bard, A.J., *J. Am. Chem. Soc*., 1989, vol. 111, p. 8901.
35. Chen, B.E., Liu, H.C., Sun, X.X., and Yang, C.G., *Mol. BioSyst*., 2010, vol. 6, p. 2143.
36. Kumar, R.S. and Arunachalam, S., *Polyhedron*, 2006, vol. 25, p. 3113.
37. Sarkar, S., Mukherjee, T., Sen, S., et al., *J. Mol. Struct*., 2010, vol. 980, p. 117.
38. Chen, L.M., Liu, J., Chen, J.C., et al., *J. Inorg. Biochem*., 2008, vol. 102, p. 330.
39. Zhang, N, Fan, Y.H., Bi, C.F., et al., *J. Coord. Chem*., 2013, vol. 66 p. 1933.